J. Basic. Appl. Sci. Res., 2(1)714-722, 2012

ISSN 2090-4304
Journal of Basic and Applied Scientific Research
www.textroad.com

Eigen Frequency Analysis of a Capacitive Micro-Beam Resonator Considering Residual, Axial Stresses and Temperature Changes Effects

Shiva Valilou

Department of Mechanical Engineering, Shabestar Branch, Islamic Azad University, Shabestar, Iran

ABSTRACT

This paper deals with the analysis of eigen frequency in a fixed-fixed micro-beam resonator considering effects of the tensile or compressive residual stresses, axial stress and temperature changes. Non linear governing differential equations of static deflection of the micro-beam using Euler-Bernoulli beam theory has been derived, and linearized using a step by step linearization method. The obtained linearized differential equation has been discretized using a Galerkin weighted residual method. The equation of small oscillations about electrostatically deflected position has been derived and solved using a Galerkin based reduced order model. The results show that owing to different applied voltage, residual stress and axial stress and temperature changes, the resonance frequency of the resonator is changed. Obtained results show that negative temperature changes and tensile residual stresses increase the first natural frequency and compressive residual stresses and positive temperature changes vice versa. Axial stress increases the first resonant frequency and its effect is more considerable when the applied DC voltage is close to the pull-in voltage.

KEY WORDS: MEMS resonator, pull-in voltage, residual stress, axial stress, temperature changes.

1. INTRODUCTION

Today because of the advantages of electrostatic MEMS switches, favorable scaling property, low power consumption, low cost, relative ease of fabrication and others, have led to replacing traditional electronic switching components (such as pin diodes), and have led to their being more widely applied the electrostatic MEMS switches applications in Micro-Electro-Mechanical Systems (MEMS). The electrostatic MEMS switches are one of the most important devices in such systems.

The most important issue in electrostatic MEMS switches is the pull-in phenomenon. Pull-in phenomenon is a discontinuity related to the interplay of the elastic and electrostatic forces when the electrostatic forces is related to the applied voltage, thus the specific applied voltage that leads to pull-in phenomenon may be called "pull-in voltage". In the MEMS switches, the pull-in voltages cause them to switch. Because of the micro scale of the electro MEMS switches some phenomena and factors, such as residual stress in thin films, fringing field effect, axial stress and so on, can influence the pull-in voltage. The other applications of determination of the pull-in voltage can be measuring the Young's modulus and the residual stress [1] and material properties [2] of MEMS switches or any micro-electro-mechanical structures such as: cantilever Microbeams, fixed-fixed Microbeams and clamped microdiaphragm. The proposed applications make pull-in voltage a relevant aspect of the numerical prediction capabilities of the design methods when the determination of the pull-in voltage and position requires the solution of a coupled electrostatic-elastic system.

Determination of the pull-in voltage has been already investigated. Some of numerical methods are: using of lumped energy model [3], Galerkin's method whose basis functions were obtained by selecting few linear undamped mode shapes, discretization techniques for both of microstructure and electromagnetic field for 2D and 3D models such as: BEM, FEM [4] and differential quadrature method (DQM) [5], reduced order model [6], meshless local Kriging method [7], step by step linearization method [8, 9] and so on.

One of the best approaches to evaluate the pull-in voltage in MEMS switches is the examination of the stability of them due to the applied voltage. Meanwhile, the pull-in voltage causes the stability of MEMS switches to be vanished. Because of the frequency shifting occurring with increasing voltage [10], one of the best methods to study the stability of the beams and microbeams are the examination of the natural frequencies of the small flexural vibrations about the equilibrium position. The first results using this approach were gained by Shashkov [11]. Later, this approach was developed by the others such as: Ziegler, Makushin, Morris, Rezazadeh [12, 13] and the others to use in the similar problems. Brusa et al. [14] developed an approach to calculate the frequency of the lumped electrostatic microbeam respect to its equilibrium position due to a specific applied voltage.

***Corresponding Author:** Shiva Valilou, Department of Mechanical Engineering, Shabestar Branch, Islamic Azad University, Shabestar, Iran.
E-mail: svalilou@yahoo.com

Due to small size, low power consumption, and ability to be integrated with microelectronics, MEMS resonators are becoming viable for use as filters in communication systems. Micromachined silicon resonators fabricated in MEMS technologies are of increasing interest for potential applications in on-chip high frequency signal manipulation, integrated circuit clock generation, and other applications based on a stable frequency reference signal and replacing bulky, off-chip ceramic and surface acoustic wave (SAW) devices. Silicon is a preferred material for high performance microresonators because of its high mechanical stiffness, excellent fatigue resistance, and compatibility with integrated circuit (CMOS) technology. Recent works have shown that it is possible to fabricate silicon MEMS resonators inside a robust, low-pressure encapsulated cavity using a CMOS-compatible process [15, 16, 17].

Types of the MEMS resonator are: MEMS capacitive resonator, MEMS magnetic resonator and piezoelectric resonator. MEMS capacitive resonator is important due to its tunable and fabrication. We are study article because of the effects of the residual stress, axial stress and different temperature changes. Residual stresses can be affected on resonance frequency. Axial stress at the resonator has the capability of high statically deformation. Applied temperatures are changed.

Since the initial demonstration of micromechanical polysilicon beam resonators [18], significant progress in resonators based on electrostatic transduction has been reported. Such devices are often used in micromachined electromechanical filters [19, 20], resonant sensors [21], oscillators [22], and similar applications where the dynamics of a micromachined structure act as a mechanical transfer function between drive and sense signals in the electrical domain. With the exception of acoustic wave devices, micro-machined piezoelectric resonators have received only limited attention, primarily due to the relative complexity of IC integration and overall device fabrication. Future advances in micromachined piezoelectric beam resonators will require compelling reasons to warrant their development alongside more established technologies such as polysilicon electrostatic resonators. Thus, the goal of this work is to investigate the modeling, fabrication, and performance of thin film piezoelectric beam resonators, and to assess the relative merits of this technology. The basic concept for these devices is similar to that of a 1969 macro-scale resonant sensor patented by Weisbord [23], in which a beam clamped to a rigid substrate at both ends is driven at its first resonant mode electrostatically, and sensed capacitively.

In spite of completed studies on the resonators, a complete study that considers residual stress, axial stress and temperature changes on mechanical behavior of a microbeam resonator simultaneously doesn't exist. Loss studies particularly on temperature changes effects, motivation became that this research to be accomplished.

2. Model Description and Mathematical Modeling

Fig.1 shows a schematic view of a fixed-fixed MEMS resonator. Assume a beam with thickness h, width b, length L, density ρ and isotropic with Young's modulus E. Suppose that x is the coordinate along the length of the beam with its origin at the left end, and $w(x)$ is the transversal deflection of the beam, defined to be positive downward.

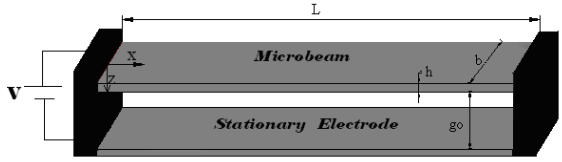

Fig.1. Schematic of the Fixed-Fixed MEM resonator

Based on the static and dynamic behavior of electrostatic MEM resonators subjected to non-uniform transverse electrostatic force, the governing equation can be expressed as [7]:

$$\widetilde{E}I\frac{\partial^4 w}{\partial x^4}+\rho A\frac{\partial^2 w}{\partial t^2}=\frac{\varepsilon b V^2}{2(g_0-w)^2} \qquad A=bh \qquad \varepsilon=\kappa\varepsilon_0 \qquad (1)$$

where κ is coefficient of different material, I is the moment of inertia of the cross-sectional area; ε is the dielectric (permittivity) of air; V is the applied voltage to the parallel plates and g_0 is the initial gap between the parallel plates. For a wide beam, the effective modulus $\widetilde{E}$ can be approximated by the plate modulus $E/(1-\upsilon^2)$; otherwise $\widetilde{E}$ is the Young's modulus E [7], where ν is the Poisson's ratio of the micro beam.

2.1. Residual stress effect

Considering the fabrication sequence of MEM resonators, the residual stress is very important and inevitable to the device. Residual stress, owing to the mismatch of both thermal expansion coefficient and crystal lattice period between substrate and thin film, is unavoidable in surface micromachining techniques. Hence accurate and reliable data of residual stress is critical to the suitable design of the MEMS devices concerned with the techniques [24]. Therefore the residual stress is a conspicuous research issue in the progress of the Microsystems Technology (MST). The effective residual stress can be calculated as follow [25]:

$$\sigma_r = \sigma_0(1-\nu) \qquad (2)$$

where σ_0 is the biaxial residual stress, σ_r is the effective residual stress. Hence, the effective axial force owing to the residual stresses can be obtained as:

$$\int_{-h/2}^{+h/2}(-Ez\frac{d^2w}{dx^2}+\sigma_r)\,b\,dz = \sigma_r\,b\,h = T_r \qquad (3)$$

2.2. Axial stress effect

When a fixed-fixed microbeam is in tension, the actual beam length L' is longer than the original length L. Although there is no displacement in the x direction at the beam ends, hence the tensile stress due to bending generates an axial force:

$$T_a = \sigma_a bh \cong \widetilde{E}bh\frac{\Delta L}{L} \qquad (4)$$

Whereas :

$$\Delta L \cong \frac{1}{2}\int_0^L\left(\frac{dw}{dx}\right)^2 dx\cdot$$

2.3. Temperature changes effects

The operating temperature of the flexible part of a MEMS resonator can be changed. These changes can occur owing to change of environmental temperature or due to heat generation because of intrinsic damping and power dissipation [ZENER]. Any change in the operating temperature of the flexible part, cause the coupled behavior of the MEMS resonator varies because the stress state is altered. Therefore, a full thermo-electro-mechanical analysis is required in identifying mechanical behavior and its implication on the resonator performance. Due to microscale of the studied microbeam Biot number is much less than 0.1 so with a good acuracy temprature distribution can be assumed uniform. Of course it must be noted that in microbeam or microplate resonators due to heat generation becaues of straine rate, a temprature gradirent will be created, but this case is not studied in this investigation**.** In the microbeam due to its fixed boundary conditions, the thermal stress in longitudinal direction can be expressed as:

$$T_T = \widetilde{E}\alpha\,\Delta T(bh) \qquad (5)$$

The governing differential equation of microbeam motion considering effects of residual, axial and temperature changes can be expressed as:

$$\widetilde{E}I\frac{\partial^4 w}{\partial x^4} - [T_r + \frac{\widetilde{E}A}{2L}\int_0^L(\frac{\partial w}{\partial x})^2 dx + T_T]\frac{\partial^2 w}{\partial x^2} + \rho A\frac{\partial^2 w}{\partial t^2} = \frac{\varepsilon b V^2}{2(g_0 - w)^2} \qquad (6)$$

The boundary conditions for the fixed-fixed micro beam are as defined below:

$$w(l,t) = 0 \quad , \quad \frac{\partial w}{\partial x}\Big|_{x=l} = 0$$

$$w(0,t) = 0 \, , \quad \frac{\partial w}{\partial x}\Big|_{x=0} = 0$$

In order to non-dimentionalize Eq. (6) following non-dimensional parameters is introduced:

$$\hat{w} = \frac{w}{g_0} \quad \hat{x} = \frac{x}{L} \quad \hat{t} = \frac{t\varepsilon}{L} \quad \varepsilon = \sqrt{\frac{\widetilde{E}}{\rho}} \qquad (7)$$

Using these non-dimensional parameters Eq. (6) takes the following form:

$$D_1 \frac{\partial^4 \hat{w}_d}{\partial \hat{x}^4} - (D_3 + D_4 \int_0^1 (\frac{\partial \hat{w}_s}{\partial \hat{x}})^2 d\hat{x} + D_5) \frac{\partial^2 \hat{w}_d}{\partial \hat{x}^2} + \frac{\partial^2 \hat{w}_d}{\partial \hat{t}^2} - D_2 \frac{V_{dc}^2}{(1-\hat{w}_s)^3} \hat{w}_d = 0 \qquad (8)$$

where

$$D_1 = \frac{h^2}{12L^2}; \quad D_2 = \frac{\kappa \varepsilon_0 L^2}{2\tilde{E}hg_0^3}; \quad D_3 = \frac{T_r}{\tilde{E}bh}; \quad D_4 = \frac{g_0^2}{2L^2}; \quad D_5 = \frac{T_T}{\tilde{E}bh}; \quad T_r = \sigma_r bh; \quad T_T = \sigma_T bh; \quad \sigma_T = \tilde{E}\alpha\Delta T$$

2.4. Dynamic Motion Equation of an Electro-statically Deflected Microbeam

In order to study microbeam motion about an electrostatically deflected position total deflection of the microbeam can be expressed as:

$$\hat{w}(x,t) = \hat{w}_s(x) + \hat{w}_d(x,t) \quad (9)$$

Assuming that a bias tuning DC voltage is applied statically, which cause the inertial terms to be vanished; equation (8) defining static deflection of the microbeam takes the following form:

$$D_1 \frac{d^4 \hat{w}_s}{d\hat{x}^4} - [D_3 + D_4 \int_0^1 (\frac{d\hat{w}_s}{d\hat{x}})^2 d\hat{x} + D_5] \frac{d^2 \hat{w}_s}{d\hat{x}^2} = D_2 \frac{V^2}{(1-\hat{w}_s)^2} \qquad (10)$$

By eliminating equation of static deflection from Eq. (8) and linearizing electrostatic nonlinear force using Calculus of Variation Theory and Taylor series expansions about static deflection the dynamic equation of small motion about electro-statically deflected position takes the following form:

$$D_1 \frac{\partial^4 \hat{w}_d}{\partial \hat{x}^4} - (D_3 + D_4 \int_0^1 (\frac{\partial \hat{w}_s}{\partial \hat{x}})^2 d\hat{x} + D_5) \frac{\partial^2 \hat{w}_d}{\partial \hat{x}^2} + \frac{\partial^2 \hat{w}_d}{\partial \hat{t}^2} - 2D_2 \frac{V_{dc}^2}{(1-\hat{w}_s)^3} \hat{w}_d = 0 \qquad (11)$$

3. Numerical Solution

3.1. Static Deflection Analysis

In capacitive tunable resonators owing to an applied DC voltage, governing equation of static deflection can be expressed as Eq. (10). Because of nonlinearity of this equation, the solution is complicated and time consuming, so in order to solve it, it is tried to linearize it. Because of considerable value of $\hat{w}_s$ respect to initial gap especially when the applied bias DC voltage is increased, the linearizing respect to the initial position may cause to appear some considerable errors. Therefore, to minimize the value of errors, a step by step increasing the applied voltage is proposed. In order to use step by step linearization method, $\hat{w}_s^i$ is considered the microbeam deflection due to an applied voltage V_i, hence a small increase of the applied voltage leads to a small change in the microbeam deflection

$$\hat{w}_s^{i+1} \to \hat{w}_s^i + \psi_s(x) \qquad (12)$$

When:

$$V_{i+1} \to V_i + \Delta V \qquad (13)$$

For step (i), will be:

$$D_1 \frac{d^4 \hat{w}_s^i}{d\hat{x}^4} - [D_3 + D_4 \int_0^1 (\frac{d\hat{w}_s^i}{d\hat{x}})^2 d\hat{x} + D_5] \frac{d^2 \hat{w}_s^i}{d\hat{x}^2} = D_2 \frac{V_i^2}{(1-\hat{w}_s^i)^2} \qquad step\ (i) \qquad (14)$$

Therefore, Eq. (8) can be rewritten as follow:

$$D_1 \frac{d^4 \hat{w}_s^{i+1}}{d\hat{x}^4} - [D_3 + D_4 \int_0^1 (\frac{d\hat{w}_s^{i+1}}{d\hat{x}})^2 d\hat{x} + D_5] \frac{d^2 \hat{w}_s^{i+1}}{d\hat{x}^2} = D_2 \frac{V_{i+1}^2}{(1-\hat{w}_s^{i+1})^2} \qquad step\ (i+1) \qquad (15)$$

Substituting Eqs. (12, 13) into Eq. (15), we have:

$$D_1 \frac{\partial^4 (\hat{w}_s^i + \hat{\psi}(x))}{\partial \hat{x}^4} - [D_3 + D_4 \int_0^1 (\frac{d(\hat{w}_s^i + \hat{\psi}(x))}{d\hat{x}})^2 d\hat{x} + D_5] \frac{d^2 (\hat{w}_s^i + \hat{\psi}(x))}{d\hat{x}^2} = \frac{D_2 V_{i+1}^2}{(1-\hat{w}_s^i - \hat{\psi})^2} \qquad (16)$$

Using Taylor's series expansion about $\hat{w}_s^i$ and applying the truncation to first order, the linear coupled electrostatic forces can be written as:

$$D_1 \frac{\partial^4 (\hat{w}_s^i + \hat{\psi}(x))}{\partial \hat{x}^4} - [D_3 + D_4 \int_0^1 (\frac{d(\hat{w}_s^i + \hat{\psi}(x))}{d\hat{x}})^2 d\hat{x} + D_5] \frac{d^2 (\hat{w}_s^i + \hat{\psi}(x))}{d\hat{x}^2} = D_2 (\frac{V_{i+1}^2}{(1-\hat{w}_s^i)^2} + \frac{2V_{i+1}^2}{(1-\hat{w}_s^i)^3} (\hat{w}_s^{i+1} - \hat{w}_s^i)) \qquad (17)$$

By substituting Eq. (17) into Eq. (16), the following equation can be obtained to calculate ψ_s:

$$D_1 \frac{d^4\hat{\psi}}{d\hat{x}^4} - (D_3 D_4 \int_0^1 (\frac{d\hat{w}_s^i}{d\hat{x}})^2 d\hat{x} + D_5) \frac{d^2\hat{\psi}}{d\hat{x}^2} - D_2 \frac{2V_{i+1}^2}{(1-\hat{w}_s^i)^3}\hat{\psi} = \frac{D_2}{(1-\hat{w}_s^i)^2}(V_{i+1}^2 - V_i^2) \quad (18)$$

The nonlinear electrostatic Eq.(8) are converted to the linear electrostatic Eq.(18), therefore implying Galerkin weigthed residual method and imposing the boundary conditions, the Eq.(18) can be discretized into nodes and by solving linear system of Algebric equations ψ_s can be obtained at a given applied voltage.

3.2. Eigen Frequency Analysis

A realistic model takes into account distributed parameters for both the structural and the electric domains. So the distributed model frequency analysis method (DMFAM) has been used to calculate the eigen frequencies of the microbeam respect to its perturbation motion evaluate the stability. Assume that the $\hat{w}_d$ is the equilibrium position of the fixed-fixed MEMS microbeam due to the applied voltage V_i . Thus, by examination of the first eigen frequency respect to its equilibrium position, the pull-in voltage can be obtained when the instability occurs. Suppose that in the equilibrium position, the microbeam can oscillates about the equilibrium position, so by substituting following equation in the Eq. (11), will be:

$$\hat{w}_d = \sum_{n=1}^{N} \varphi_n(x)\, U_n(t) \quad (19)$$

$$D_1 \sum_{n=1}^{N} U_n(t)\, \varphi_n^{(4)}(x) - (D_3 + D_4 \int_0^1 (\frac{\partial \hat{w}_s}{\partial \hat{x}})^2 d\hat{x} + D_5) U_n(t)\, \varphi_n^{(2)}(x) + \sum_{n=1}^{N} U_n^{\bullet\bullet}(t)\, \varphi_n(x) - 2D_2 \sum_{n=1}^{N} \frac{V_{dc}^2}{(1-\hat{w}_s)^3} U_n(t)\, \phi_n(x) = \varepsilon_r \quad (20)$$

By considering Galerkin based Reduced Order Model, will be:

$$D_1 \sum_{n=1}^{N} U_n(t) \int_0^1 \varphi_n^{(4)}(x)\, \varphi_j(x)\, d\hat{x} - \{D_3 + (D_4 \int_0^1 (\frac{\partial \hat{w}_s}{\partial \hat{x}})^2 d\hat{x}) \sum_{n=1}^{N} U_n(t) + D_5\} \sum_{n=1}^{N} U_n(t) \int_0^1 \varphi_n^{(2)}(x) \varphi_j(x) d\hat{x} + \sum_{n=1}^{N} U_n^{\bullet\bullet}(t) \int_0^1 \varphi_n(x)\, \varphi_j(x)\, d\hat{x}$$

$$- 2D_2 \sum_{n=1}^{N} U_n(t) \int_0^1 \frac{V_{dc}^2}{(1-\hat{w}_s)^3} \varphi_n(x)\, \varphi_j(x)\, d\hat{x} = 0 \quad (21)$$

$$\sum_{n=1}^{N} M_{nj}\, U_n^{\bullet\bullet}(t) + \sum_{n=1}^{N} (K_{nj}^{mech} - K_{nj}^{elec} - K_{nj}^{thermal} - K_{nj}^{axial} - K_{nj}^{residual})\, U_n(t) = 0 \quad (22)$$

Whereas:

$$M_{nj} = \int_0^1 \varphi_n\, \varphi_j\, d\hat{x}; \qquad K_{nj}^{mech} = \int_0^1 D_1\, \varphi_n^{(4)}\, \varphi_j\, d\hat{x}; \qquad K_{nj}^{elec} = \int_0^1 \frac{D_2\, V_{dc}^2}{(1-\hat{w}_s)^3} \varphi_n\, \varphi_j\, d\hat{x} \quad (23)$$

$$K_{nj}^{axial} = \int_0^1 (D_4 \int_0^1 (\frac{\partial \hat{w}_s}{\partial \hat{x}})^2\, d\hat{x})\, \varphi_n^{(2)}\, \varphi_j\, d\hat{x}; \quad K_{nj}^{residual} = \int_0^1 D_3\, \varphi_n^{(2)}\, \varphi_j\, d\hat{x}; \quad K_{nj}^{thermal} = \int_0^1 D_5\, \varphi_n^{(2)}\, \varphi_j\, d\hat{x}$$

By solving the top equation, we will be achieving matrice that by appointing determinant equal zero, we will be achieving the value of the natural frequency.

4. Numerical results and discussion

As an illustration, a silicon beam is considered with the geometric and material constants list in Table 1.

Table1-Geometrical and material properties of the MEMS resonator

Parameter	Parameter value
Width	50μm
Height	3μm
Initial gap(g0)	1μm
Poisson's ratio	0.06
Coefficient of elasticity	169GPa
Density	$2331\,kg/m^3$
Coefficient air dielectric(ε0)	$8.854187\times10^{-6}F/m$
Length	350μm
α (Si)	2.6×10^{-6} k^{-1}

Considering the effects (residual and axial stress and temperature changes effects), the results are compared with the results predicted by employing Matlab, to demonstrate the feasibility of the step by step linearization method for solving mentioned equation. For finding the best step size for applying voltage and number of grid points for the finite element method, some sample grid points with step size for the applying voltages are used. The results are listed in Table 2.

Table 2- Looking for the optimum grid size ($\delta V = 0.1$)

number of mode shapes	N=1	N=2	N=3	N=4	Co Solve Simulation [12]
pull-in voltage	19.7	20.1	20.2	20.2	20.2

From the above tabulation, it can be easily found out that the optimum grid size to obtain convergence with three digits is $N = 3$.

The effect of residual stresses and pull-in voltage on the natural frequency of a micro-beam resonator with the same properties as listed in Table 1 has been represented in Fig2.

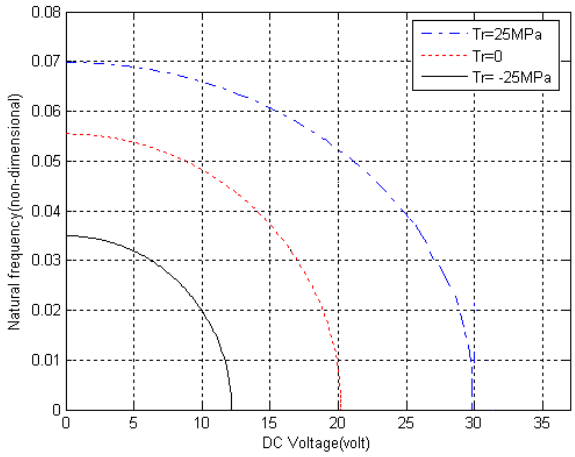

Fig2-first natural frequency changes considering different residual stresses ($T_a = 0,\ \Delta T = 0$)

As shown in fig2, considering the tensile residual stress ($T_r > 0$), the first natural frequency will be increased and considering the compressive residual stress ($T_r < 0$), the first natural frequency will be decreased. So, effect of the axial stress on the pull-in voltage and first natural frequency of the micro resonator has been represented in Fig3.

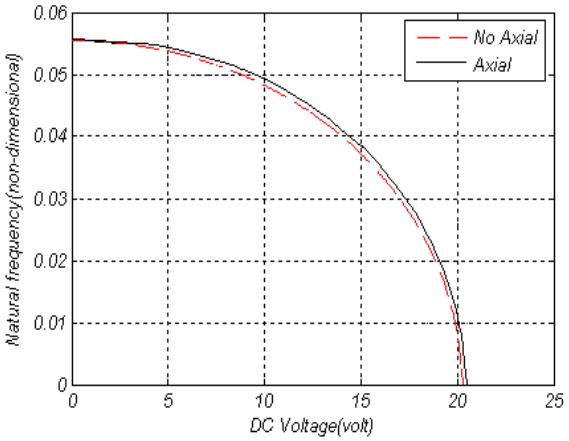

Fig3-first natural frequency changes with and without axial stress ($T_r = 0,\ \Delta T = 0$)

As shown in fig3, axial stress increases the first resonant frequency and its effect is more considerable when the applied DC voltage is close to the pull-in voltage. Effects of temperature changes on the pull-in voltage and first natural frequency have been represented in Fig4.

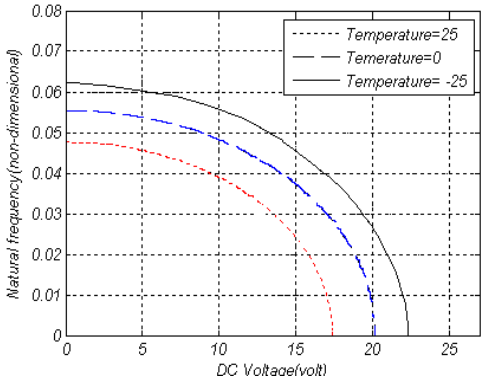

Fig4- first natural frequency changes with considering different temperature changes ($T_r = 0,\ T_a = 0$)

As shown in fig4, considering positive temperature changes, the first natural frequency will be decreased and considering negative temperature changes, the first natural frequency will be increased. If in case considering effects tensile residual stresses, axial stresses, figure will be for different temperature changes as follow:

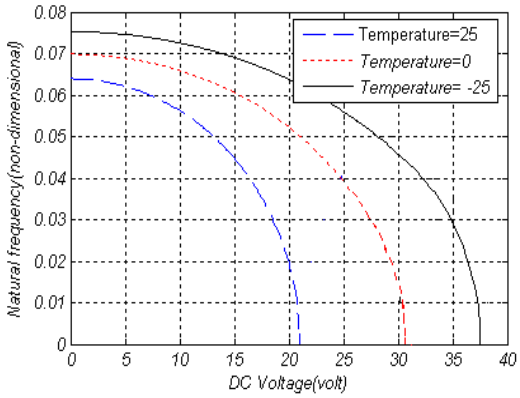

Fig5-eigen frequency changes with considering axial and tensile residual stress $T_r > 0$ *and different temperature changes*

As shown in fig5, for positive temperature changes, eigen frequency will be decreased and for negative temperature changes, eigen frequency will be increased. If in case considering effects compressive residual stresses, axial stresses, figure will be for different temperature changes as follow:

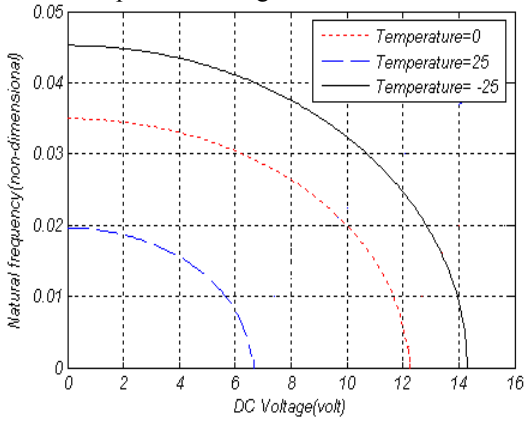

Fig6- eigen frequency changes with considering axial and compressive residual stress $T_r < 0$ *and different temperature changes*

As shown in fig6, for positive temperature changes, eigen frequency will be decreased and for negative temperature changes, eigen frequency will be increased.

5. Conclusions

The governing equations of the statical and dynamical behavior have been derived by considering the tensile or compressive residual stresses, axial stresses and temperature changes effects. At the statical state, linearized equations with Step by Step Linearization Method (SSLM) and solved yielding equations by Galerkin method. At the dynamical state, used for solving from Galerkin-based reduced-order model. Obtained results show that negative temperature changes and tensile residual stresses increase the first natural frequency and compressive residual stresses and positive temperature changes viceversa. Axial stress increases the first resonant frequency and its effect is more considerable when the applied DC voltage is close to the pull-in voltage. Too, show that for tensile and compressive residual stresses, axial stresses, if negative temperature changes be, the first natural frequency will be increased and if positive temperature changes be, the first natural frequency will be decreased.

REFERENCES

[1]. Osterberg P. M., Senturia S. D., “M-test: a test chip for MEMS material property measurement using electrostatically actuated test structure”, Journal of Microelectromechanical Systems 1997, 6(2); 107-18.

[2]. Chan E., Garikipati K., Dutton R., “Characterization of contact electromechanical through capacitance-voltage measurements and simulations”, Journal of Microelectromechanical Systems 1999, 6(2), 107-18.

[3]. Osterberg P. M., Yie H., Cai X., White J., Senturia S., “Self-consistent simulation and modeling of electrostatically deformed diaphragms”, Proceeding of the IEEE Conference on Micro Electro Mechanical Systems, Osio, Japan,

[4]. Mukherjee S. R., “Dynamic analysis of micro-electromechanical system”, International Journal of Numerical Methods in Engineering, vol. 39, pp. 4119– 4139, 1996.

[5]. Kuang JH., Chen CJ., “The nonlinear electrostatic behavior for shaped electrode actuators”, International Journal of Mechanical Science 47 (2005), 1172-1190.

[6]. Younis M. I., Abdel-Rahman E. M. and Nayfeh A., “A reduced order model for electrically actuated microbeam-based MEMS”, Journal of Microelectromechanical Systems, vol. 12, no. 5, pp. 672– 680, 2003.

[7]. Rezazadeh Gh., Tahmasebi A. and Zubtsov M.," Application of Piezoelectric Layers in Electrostatic MEM Actuators: Controlling of Pull-in Voltage", Journal of Microsystem Technologies, Vol.12, No. 12. , pp 1163-1170, 2006.

[8]. Rezazadeh Gh., Khatami F. and Tahmasebi A., "Investigation of the torsion and bending effects on static stability of electrostatic torsional micromirrors", Journal of Microsystem Technologies, Vol.13, No. 7. , pp 715-722, 2007.

[9]. Wang QX., Li H., Lam KY., Gu YT., “Analysis of microelectromechanical systems (MEMS) by meshless local kriging (LOKRIGING) method”, Journal of Chinese Institute of Engineers, Vol. 27, No. 4, pp. 573-583 (2004).

[10]. Lee K., Kim K. and Youn C., “Numerical approach for frequency-shifting analysis of electrostatic micro-mechanical actuator.” In Proc. of the Symposium on Design Test Integration Packaging MEMs/MOEMs, SPIE, Cannes, 2001, pp. 90–98.

[11]. Shashkov I. E., “Influence of twist on Stability and critical speed of shaft” Applied Mechanics, 1939, No2.c79-1404.

[12]. Rezazadeh Gh., Svetlitsky V. A., “Fluid Flow Impact on Dynamic Stability of the straight Rod Under Compression and Torsion Conditions”, Journal of VESTNIK of BMSTU, No.3, 1997.

[13]. Rezazadeh Gh., Svetlitsky V. A., “Fluid Flow Impact on Static Stability of the straight Rod Under Compression and Tortion Conditions”, Journal of Academy of Science of Russia, Mechanics of Solids, No. 3,1997.

[14]. Brusa E., Bona F. De, Gugliotta A. and Som`A .A., "Modeling and Prediction of the Dynamic Behaviour of Microbeams Under Electrostatic Load", Analog Integrated Circuits and Signal Processing, 40, 155–164, 2004.

[15]. Candler, R.N., et al., "Single wafer encapsulation of MEMS devices". IEEE Transactions on Advanced Packaging, 26(3), 2003.

[16]. Partridge, A., et al. "New thin film epitaxial polysilicon encapsulation for piezoresistive accelerometers". At MEMS '01, 2001. Interlaken, Switzerland.

[17]. Candler, R.N., et al. "Hydrogen diffusion and pressure control of encapsulated MEMS

Resonators". At TRANSDUCERS '05, 2005.

[18]. Howe R.T., Muller R.S., "Integrated resonant-microbridge vapor sensor", IEEE Int. Elec. Devices Meeting Technical Digest (1984) 213±216.

[19]. Nguyen C.T.-C., "High-Q micromechanical oscillators and filters for communications", in: Proceedings of the IEEE International Symposium on Circuits and Systems, 1997, pp. 2825±2828.

[20]. Wang K., Nguyen C.T.-C.," High-order micromechanical electronic filters", in: Proceedings of the 1997 IEEE International MEMS Workshop, 1997, pp. 25±30.

[21]. Roessig T., Howe R.T., Pisano A.P., "Surface micromachined resonant accelerometer", Proc. Transducers'97 2 (1997) 859±862.

[22]. Nguyen C.T.-C., Howe R.T., "An integrated CMOS micromechanical resonator high-Q oscillator", IEEE J. Solid-State Circuits 34 (4) (1999) 440±455.

[23]. Weisbord L., "Single beam force transducer with integral mounting isolation", US Patent # 3 470 400, 1969.
[24]. Mukherjee T., Fedder G. K. and White J., “Emerging simulation approaches for

micromachined devices,” IEEE Trans. Comput.-Aided Design Integr.Circuits Syst., vol. 19, pp. 1572–1589, Dec. 2000.

[25]. Senturia S.D., “CAD challenges for microsensors, microactuators, and microsystems,” Proc. IEEE, vol. 86, pp. 1611–1626, 1998.